

Review

New Laser Fusion and Its Gain by Intense Laser

Kazuo Imasaki * and Dazhi Li

Institute for Laser Technology, 2-6 Yamada-oka, Suita, Osaka, Japan; E-Mail: dazhi_li@hotmail.com

* Author to whom correspondence should be addressed; E-Mail: kzoimsk@ile.osaka-u.ac.jp;
Tel.: +81-6-6879-8739; Fax: +81-6-6878-1568.

Received: 5 April 2010 / Accepted: 28 April 2010 / Published: 8 June 2010

Abstract: The feasibility of a new approach of laser fusion in plasma without implosion has been proposed and is discussed using an intense laser. The cross section of the nuclear reaction is increased by enhancing the penetrability of nuclei through the Coulomb barrier. In this approach, an intense laser field of more than 100 PW was required to distort the Coulomb barrier to obtain enough penetrability. An energy gain even with Deuterium-Deuterium (D-D) reaction can be obtained using this scheme in Deuterium plasma. A reactor with neutron and direct conversion of charged particle beam individually is proposed. Charged particles from D-D reaction are guided to the end of the reactor and are directly converted by a MHD scheme into electric energy. The energy recovery rate is high and requires a small amount of laser energy, which may make the energy cost cheaper than that of a fission reactor.

Keywords: laser fusion; nuclear reaction; nucleon; nuclear potential

1. Introduction

The final goal of fusion research is to combine both clean and the sustainable energy to get economical energy. Today, laser fusion has been developed, and ignition may be expected in the near future. However, there are many issues for commercial reactors in ICF as the cost of complicated and precise pellet targets require a large laser with a high repetition rate. Therefore, it is hard to satisfy the economical conditions even though we can achieve ignition and obtain a gain.

From this point of view, we proposed a new laser fusion and we have investigated the feasibility of the approach of a laser driven nuclear reaction using intense laser field along this concept at laser peak [1]. Here we have added and summarized an additional penetration around the laser peak and focusing

point. The intense laser field distorts the Coulomb barrier, which enhances the tunneling. This forms the cloud by the tunneled nucleon and they react when they meet each other. This is a non-Gamov nuclear reaction. A more than 100 PW laser is required to distort the Coulomb barrier to obtain enough penetrability for tunneling, however, in this way, the total energy of the laser and the cost of the energy are significantly reduced. In this article, the model and the gain for Deuterium-Deuterium (D-D) reaction in this way are discussed.

The concept of thermonuclear fusion was first presented by Gamov and Teller [2]. Since this research, many investigations of thermonuclear fusion have been studied over the time. A well-known reaction cross-section was obtained from LANL experiments and the reaction rate was obtained from this as Maxwell distribution.

Concerning the laser fusion, Nuckolls and Livermore proposed an attractive way of compression by the implosion and since then, high performance lasers have been developed [3]. However, an ignition is required in this case. However, we need the symmetry and the uniformity with high accuracy for irradiation, as well as a high power to ignite; this leads to an indirect target of which implosion efficiency is not good. So we need an enormous laser.

For this purpose, intense laser technology is rapidly growing. Using such lasers, we have proposed the feasibility of a new approach of laser-induced nuclear reaction using an intense laser field. Such an intense laser field distorts the Coulomb barrier, which enhances the tunneling. This forms the cloud by the tunneled nucleon and they react when they meet each other. This is a non-Gamov nuclear reaction and the cross section is rather large, although more than a 100 PW laser was required to distort the Coulomb barrier to obtain enough penetrability for tunneling [3].

In this way, ignition is not an essential point as usually required in ICF as a first point. So we may be free from several serious issues such as symmetry and uniformity of lasers, though it is necessary to propagate in the uniform plasma for the intense laser below the critical density. A low price gas target and smaller energy laser is used, these lead to an energy cost much lower than that of usual ICF. The high repetition of the smaller laser is easier to achieve. This fact drastically reduces the laser energy cost to result in an actual gain and shows an important characteristic of this approach. The energy cost may be cheaper than that of the fission reactor in the real and future cases.

Another point of this approach is the increment of fusion reaction rate due to the tunneling and cloud formation. The detail is discussed in Section 5. We can expect a reactor using deuterium plasma.

In this article, modeling and assumptions for this scheme are discussed in Section 2 and potentials of nuclei with laser field are estimated in Section 3. Penetrability of nucleon through the Coulomb barrier and formation factor of nuclei with tunneled nucleon as a cloud are discussed in Section 4. Energy gain by D-D reaction in plasma in this scheme is discussed in Section 5 and Section 6 is a brief note for this reactor in this way. The summary and conclusion of the article are written in Section 7.

2. Modeling and Assumptions

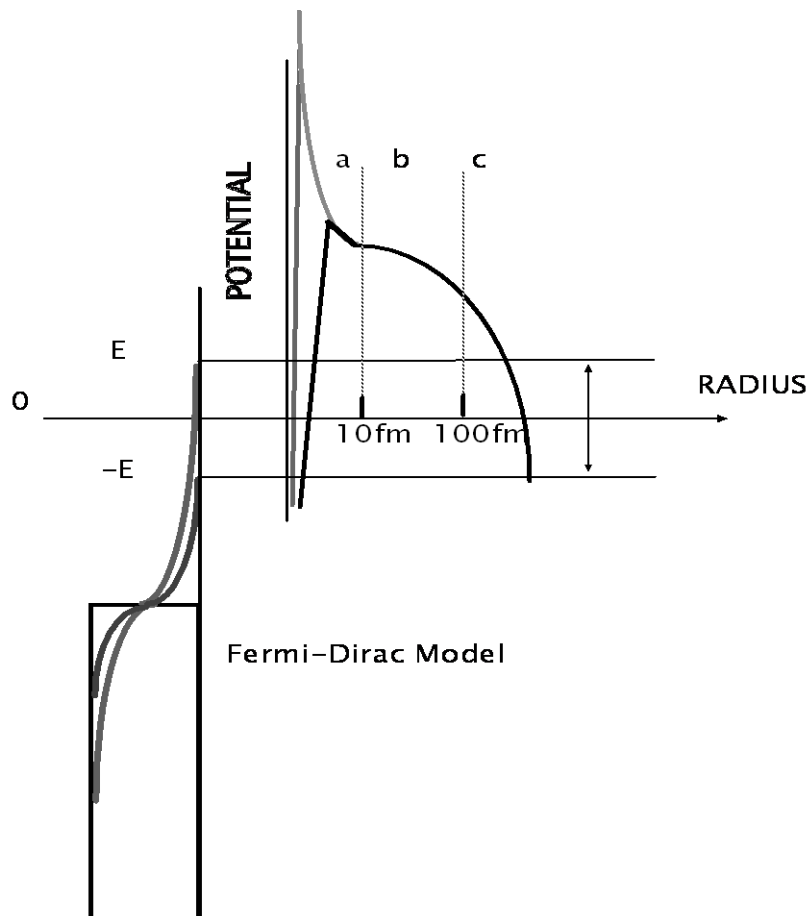
Low temperature plasma with a density slightly lower than the solid laser cut-off is considered in this model. Around the center of the nuclei, there is a well of nuclear potential with radius of 5 fm, which is shown by the region of the gray line in Figure 1. However, in the actual case, there are mesons for nucleon, which work as an attractive force. Due to mesons, the nuclear potential can be shifted as

seen by the black solid line in Figure 1. This effect is included here in the simple calculation of penetrability.

The Coulomb barrier is dominant in the outer region, and this is schematically shown as region b in Figure 1. In the normal case without the intense laser, the field is decayed away with D^{-1} . Here, D is a distance from the nuclear core center.

At the foot of the Coulomb barrier with intense laser, the laser field becomes dominant. This is shown as region c of Figure 1. This shows a picture at peak laser field. In the laser-dominated region, the field is oscillated with the laser field. The distribution of nucleon is along the Fermi model shown in Figure 1. The intense laser is focused, and injected into the plasma as a Gaussian beam. Then, this laser can propagate through the plasma. During this, the intense field by the laser is applied along the center of the laser path. This field distorts the Coulomb barrier in each peak of each laser cycle, which promotes the tunneling. The tunneled nucleon forms a cloud of probability of de Broglie wave of nucleon. The cloud expands with group velocity v_g of the tunneled nucleon. This expansion is kept in the oscillating laser field with the energy of Heisenberg uncertainty. Tunneled nucleons form a cloud around nuclei. When the cloud of tunneled nuclei meet each other, they immediately make a compound nucleus and react as in a usual nuclear reaction. This takes place during the laser pulse.

Figure 1. Typical potential of nucleus with intense laser. Gray line = well of nuclear potential with radius of 5 fm; black line = nuclear potential shifted due to mesons; b = region where Coulomb barrier is dominant; c = region where laser field is dominant.

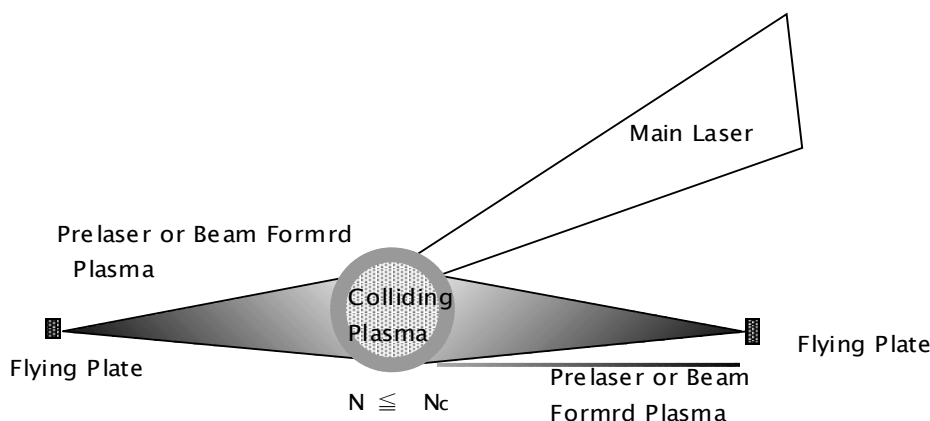


After the laser pulse, the nuclei with the clouds diffuse away so the probability of meeting each other rapidly decreases and reactions eventually reduce. Nucleon at high-level potential can survive in the Coulomb potential barrier and can penetrate through. Nucleon at low-level potential decay and are stopped to return back to a core center. This process is repeated many times in the laser power peak, most of the nuclei are tunneled through the procedure.

Basic assumptions in this model are noted as follows [4]:

1. Plasma is formed with density up to $10^{21}/\text{cm}^3$, which is below the cut off density of 1 micrometer wavelength of solid state laser. For simplicity, we assumed plasma density to be uniform and charge neutral, and non-linear interaction was not induced. There are several ways to make plasmas with sufficient relative velocity. For an example, after the injection of a jet of fuel from opposite sides in the reactor center, the plasma is irradiated by an appropriate laser pulse from each end before the main pulse. Plasma with a sufficient relative velocity is produced. The plasma shape may be several tens of centimeters in length and several cm in radius. Such plasma is formed and accelerated by lasers or ion beams on actual application [5]. Laser irradiation makes a mm radius active area as shown in Figure 2.

Figure 2. Model for the nuclear reaction with a cloud around nuclear core.



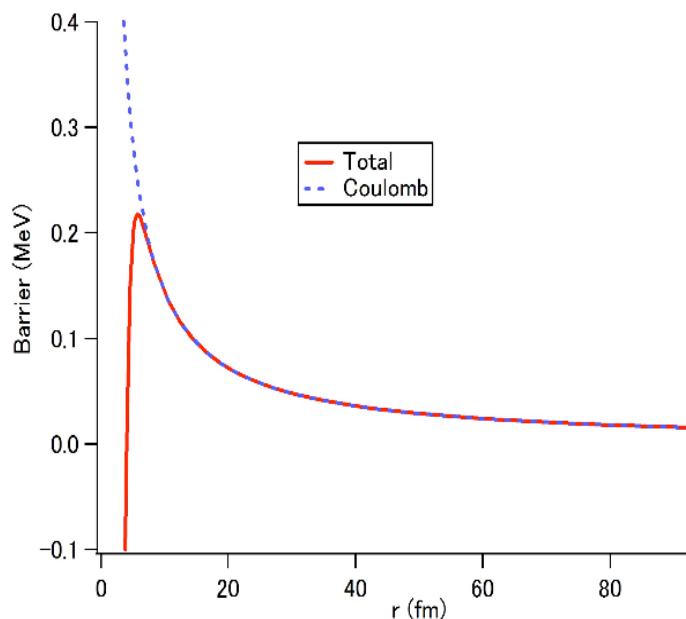
2. The wavelength of the laser is $1.06 \mu\text{m}$. Today, laser technology for a solid-state laser of $1 \mu\text{m}$ wavelength is well developed for laser fusion. So the solid-state laser is the first candidate for this intense laser to EW output. Their efficiency and repetition rate are improved as a laser fusion driver gradually. An optimal wavelength for this scheme may be a shorter wave as 2 or 3 omega and is discussed elsewhere.

3. In the first stage without the intense laser, nucleons are trapped in nuclear potential and hit the inner wall of the Coulomb barrier in many times of laser power peak with nucleon kinetic energy up to a few million eV. The typical round time from the motion is estimated to be 10^{-20} to 10^{-21} sec, so this is much shorter than the laser peak period. This is shown in Figure 3 for normal nuclei. The usual thermonuclear fusion reaction is induced by nuclei with high velocity to run up the Coulomb potential barrier and meet the tunneling nucleon (dashed line) in the Coulomb potential barrier.

4. One of main issues for penetrability is the nucleon energy level. Nucleon distribution in the core is determined by the Fermi-Dirac model, as shown in Figure 1. The nucleon in Coulomb barrier is free from the nuclear potential so the energy level of the nucleon cannot be determined around the foot of

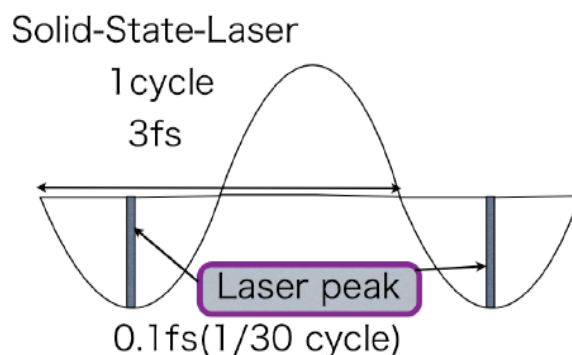
the barrier simply. In this article, energy level E is assumed for typical level and is varied from +5 to 1 keV. We will discuss this in a later section.

Figure 3. Potential and Coulomb barrier of normal nuclei.



5. A typical relation of laser waveform and its defined field peak are shown in Figure 4. Around the laser peak per cycle, the laser field distorts the nuclear Coulomb barrier to promote tunneling. So the summarization for tunneling is calculated including the laser field. Then such tunneled nucleons form a cloud around nuclei. Therefore, the cycle number corresponds with the formation factor of cloud. This is repeated every cycle in a laser pulse of more than a hundred fs.

Figure 4. Laser cycle and peak power waveform



6. A gaussian laser beam of 2 m in diameter with annular shape for a long and tight focusing is applied. The first sixth of the laser pulse is rise time. The power crest is two-thirds of the laser pulse and it is an effective period of laser tunneling. After this, the laser pulse decays within one-sixth of the pulse. It is an enough time to tunnel out of the region b of Figure 1.

7. Clouded nuclei are piled up through the laser pulse. Cloud life may be limited by a pion lifespan of 10 ns in free space, but it is also limited by the effective laser pulse due to the diffusion in the

focusing area for the nuclear reactions. The nuclear reaction decreases rapidly after the laser pulse which may be shorter than the pion life span. So we set the effective reaction duration laser pulse.

3. Nuclei in Laser Field

3.1. Coulomb Barrier and Nuclear Potential

At the center of nuclei, there are mesons to combine nucleons. They reduce the Coulomb potential and make an attractive force to the nucleons around the center. This force is estimated by nuclear potential as shown in Figures 1 and 3. A simple Coulomb potential is shown as a dashed line that we used in a model in Figure 3. Precise total nuclear potential is estimated by Yukawa model with appropriate mesons. The difference was recognized around the center at 5–10 fm when the model was set and a solid line shown in Figure 3 was obtained. The initial value of barrier around the core is reduced significantly, which is effective for tunneling and allows penetrability to be enhanced.

3.2. Coulomb Barrier with Laser Field

The nucleon wave traveling through the Coulomb barrier realizes an exponential decay, and finally it is reflected in most cases. When the intense laser is applied, the field in the foot of the Coulomb barrier is distorted at the laser intensity peak. Then, the possibility to penetrate the barrier increases.

A is the field of applied laser and can be written as [1]:

$$A(V/m) = 2.7 \times 10^3 I^{1/2} (W/cm^2) \quad (1)$$

Here, I indicates the power density of the laser. With a simple model, the potential induced by the laser field can be written as $\varphi_L = -Er$, where the field can be given as $E = A \sin(\omega t)$. Then, we have the total nuclear potential with mesons, Coulomb barrier and laser as [1]:

$$\varphi_{total} = \frac{Z_1 e}{4\pi\epsilon_0 r} + \varphi_L - V_0 \frac{e^{-\frac{r}{r_0}}}{r} = \frac{Z_1 e}{4\pi\epsilon_0 r} - A \sin(\omega t) r - V_0 \frac{e^{-\frac{r}{r_0}}}{r} \quad (2)$$

The first term is the Coulomb field, the second term is the laser field and the third term is the nuclear potential with pions. Here, we use Yukawa potential from pion, which can be written using $V_0 = 109$ MeV, r a distance in fm and $r_0 = 1.13$ fm in the usual case.

Let us consider two extreme cases for this potential at the laser peak. We can derive the following equations from Equation 2.

One is

$$U_1 = \left(\frac{Z_1 e}{4\pi\epsilon_0 r} - Ar \right) Z_2 e - V_0 \frac{e^{-\frac{r}{r_0}}}{r} \quad (3)$$

and the other is

$$U_2 = \left(\frac{Z_1 e}{4\pi\epsilon_0 r} + Ar \right) Z_2 e - V_0 \frac{e^{-\frac{r}{r_0}}}{\frac{r}{r_0}} \tag{4}$$

In Equation 3, one can decrease the barrier. Let us focus on U_1 providing $Z_1 = Z_2 = 1$, then we calculate and figure out U_1 .

Under this assumption, each line in Figure 5 indicates the calculated results of fields with various laser intensity peaks in Equation 3.

Figure 5. Nuclear potential and Coulomb barrier with various laser power intensities from 10^{28} W/cm^2 to 10^{24} W/cm^2 .

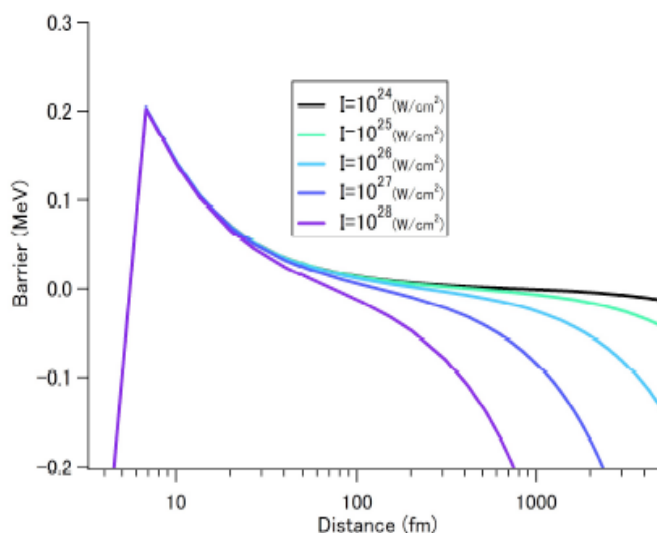
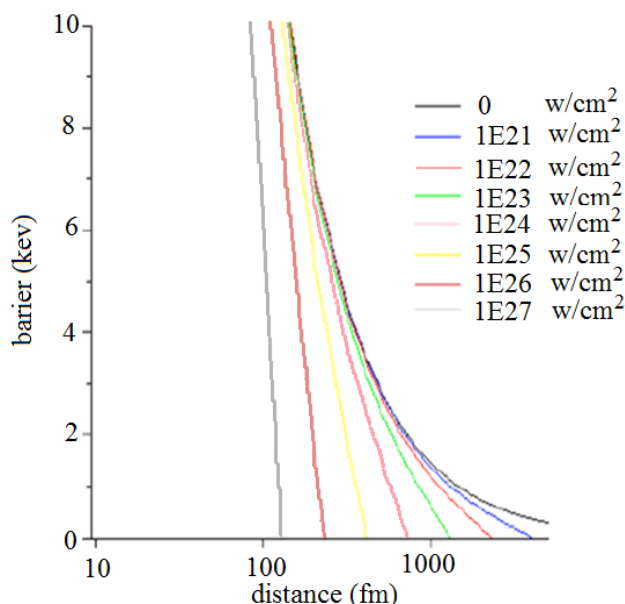


Figure 6 indicates the details of the barrier potential around grand level with various lasers. In the actual case, tunneled nucleons travel through the barrier and come out to the free space, which makes a cloud.

Figure 6. The details of the barrier potential around grand level with various lasers.



3.3. Penetrability and Formation Factor

The transmission rate T is calculated as follows using a potential of nuclei discussed in section 3.2. Then the transmission rate of the nucleon passing through the barrier is expressed as [4]:

$$T = \exp(-2 \int_R^{R_1} \beta(x) dx) \tag{5}$$

where

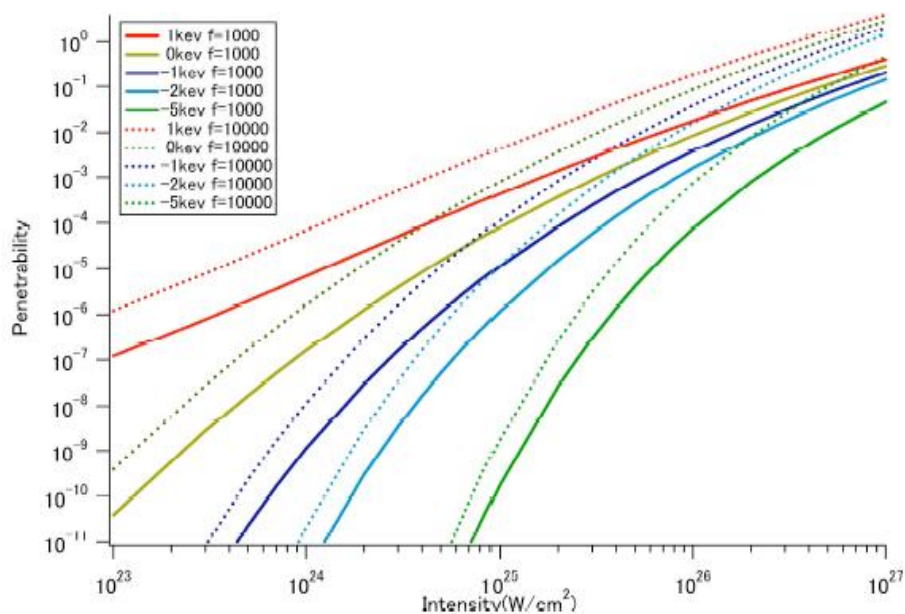
$$\beta(x) = \left(\frac{2m}{\hbar^2}\right)^{\frac{1}{2}} [U_1(r) - E]^{\frac{1}{2}} \tag{6}$$

Here, $m = 938.28 \text{ MeV}/c^2$ is for proton, and $\hbar = 6.58217 \times 10^{-16} \times 10^{-6} \text{ MeV} \cdot \text{s}$. A simple transmission rate T is modified, and penetrability P is defined as

$$P = fT \tag{7}$$

Here, f is a collision time of the nucleon with the inner wall produced by the nuclear potential and the Coulomb barrier. Setting the nuclear potential radius 5 fm as in the usual case, one can estimate f to be more than 10,000 through nucleon kinetic energy corresponding to 1 MeV during the laser peak. In the actual case, E in Equation 6 corresponds to this relation of energy level of the nucleon. It should be determined by experiments, but for this simple calculation in this paper, we use the parameters 0 eV to 10 keV. Then, the penetrability is calculated as shown in Figure 7 from the Equations 5, 6 and 7 with various parameters.

Figure 7. Calculated penetrability with laser peak power.



Compared with the quantum well model, significant enhancement was observed in the region of laser power around 10^{24} to $10^{26} \text{ W}/\text{cm}^2$. This is due to nuclear potential effect around the center. A typical velocity of a nucleon in the core is estimated as 10^4 to $10^5 \text{ m}/\text{s}$. From the velocity, a traverse time for 1000 fm is estimated to be 0.01 to 0.1 fs. Therefore, the penetrability obtained in Equation 5 is valid in our case during the laser peak.

Here we define F as a formation factor of cloud of a tunneled nucleon after penetration. The probability of the formation of a cloud can be written as

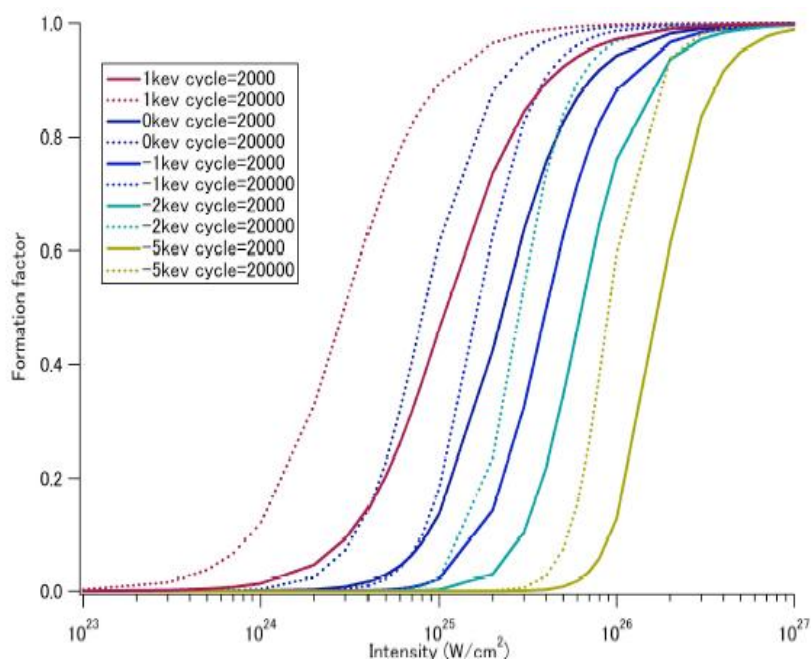
$$F = P \times N_c$$

Here N_c is a cycle number of laser pulse crest, which can be taken as 200 to 2000 in this case. When F is approaching to one, the saturation with depletion of nuclei and so on will be taken place. For the calculated result shown in Figure 8, this effect is included. In this region, the F_s for saturation level can be roughly written using F as

$$F_s = F / (F + 1) \tag{8}$$

Typical results obtained with Equation 8 are shown in Figure 8. Here, two cases of cycle number for 2000 in 900 fs pulse length and 20,000 in 10 ps of pulse length as a various pulse cases are shown.

Figure 8. Formation factors of cloud for long pulse cases.



3.4. Nucleon Tunneling Energy Level

Nucleon energy level is an essential point for tunneling. We have estimated this by two ways. In the usual case for high temperature fusion, cross section is obtained as is shown as a dot line in Figure 9. The decay rate in low temperature region, the cross section agrees with $Jr^2 \exp T$: here J is an adjustable parameter and r is the radius of nuclei. This corresponded well to the curves between 2 to 5 keV below the 10 keV region.

This result shows that the energy level of a nucleon in this region might be between 2 to 5 keV.

Figure 10 shows simple results of Heisenberg uncertainty of the nucleon energy and the Coulomb barrier level with laser around ground level shown in Figure 9. Heisenberg uncertainty gives a maximum energy of a nucleon during the tunneling. This result corresponds quite well to the result of Figure 9.

Considering these two results, the energy level for a nucleon to penetrating the Coulomb barrier is several keV in several hundred fm in distance from the center core with a laser intensity of more than 10^{23} W/cm².

Figure 9. Natural nuclear potential without laser.

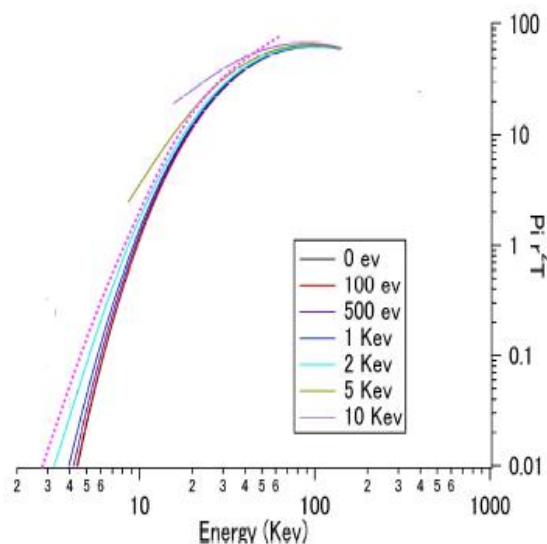
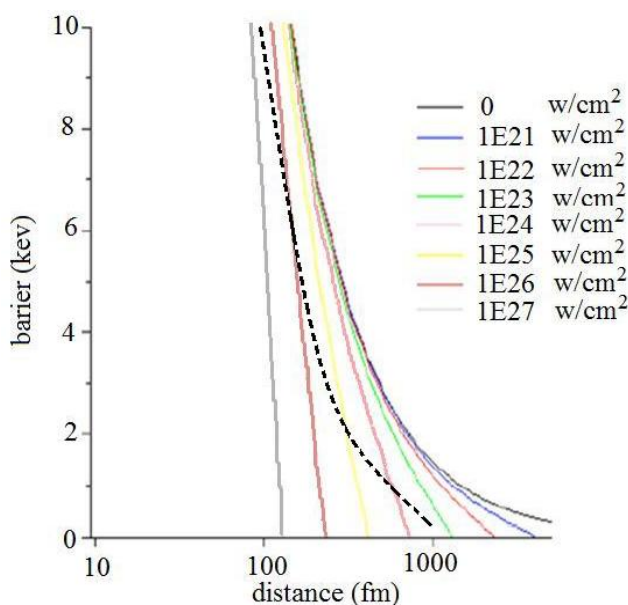


Figure 10. Heisenberg uncertainty of the nucleon energy during the tunneling and Coulomb barrier level with laser in Figure 5.



4. Nuclear Reaction Rate

Here the formation factor is fixed as $f = 0.3$. The laser intensity and pulse length are fixed as $10^{24.5}$ W/cm² and 1 ps. These are typical numbers for the scheme shown in Table 1.

When clouds meet each other, nuclear reactions take place. From this model, the reaction rate is estimated and is shown in Figure 11. A radius of cloud is calculated as

$$r = V_g \langle t \rangle \tag{9}$$

Here, V_g is the group velocity of de Broglie wave of nucleon. $\langle t \rangle$ is a average time of cloud holding in the reacting area. In the unit period of t , each nucleus has a relative velocity of V_r with cloud density of n_c . We introduce r , a radius of the cloud diffusion area of tunneled nucleon wave during the laser pulse of 1 to 100 ps.

Thereafter, the reaction rate R_r in this model of Figure 10 is written as

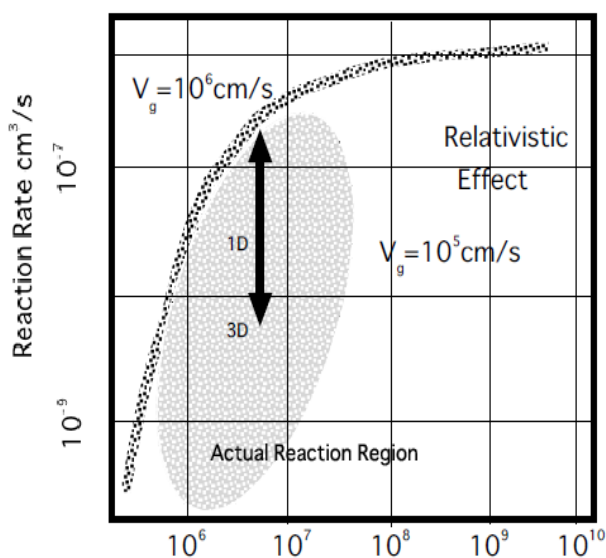
$$R_r = F_1 F_2 \pi r^2 v_r \tag{10}$$

In this equation, F_1 and F_2 are formation factors of laser tunneling nuclei for n_1 and n_2 of two species. n_1 and n_2 are number density of reacting plasma.

In the unit period of t , each nucleus has a relative velocity of V_r with a cloud density of n_c . This is given by the group velocity of the tunneled nucleon wave and is estimated to be 10^6 cm/s. So r is 10^{-6} cm in our case. v is the relative velocity of nuclei to each other by the thermal motion or differential accelerated particle velocity by laser. We use a typical velocity of 2×10^6 cm/s.

Then the reaction rate can be calculated for a density of plasma using parameters of relative velocity as shown in Figure 11. There is a density limit for laser beam propagation. So the density of plasma should be less than this parameter, which is shown in Figure 11.

Figure 11. Relative Velocity for Reaction Rate.



In the actual case, we can make the particle relative velocity much higher than usual thermal velocity when we use a pre-pulse or double pulse of laser or particle beam. When we use a laser to irradiate from opposite sides, we can obtain a relative velocity more than 10^8 cm/s, just before the main pulse in this case. Here, we can use a usual reaction model between the molecules shown in Figure 12. A Gaussian Intense laser with tight focusing is injected into such plasma. Figure 13 shows a contour of laser intensity in such plasma.

Figure 12. Model for nuclear reaction with a cloud around the nuclear core.

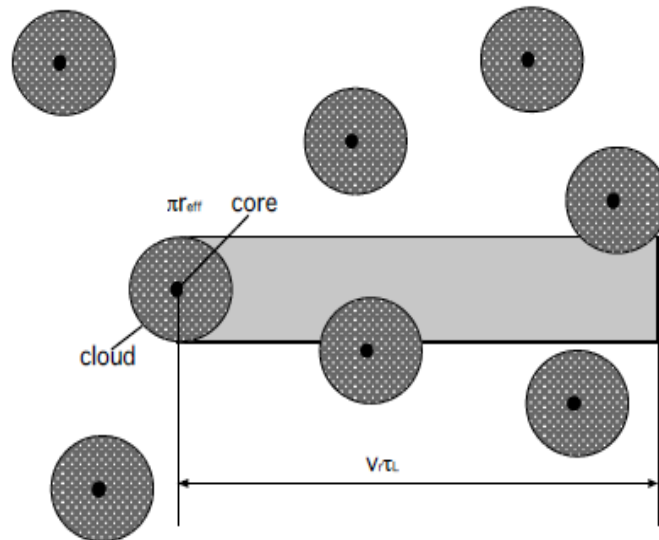
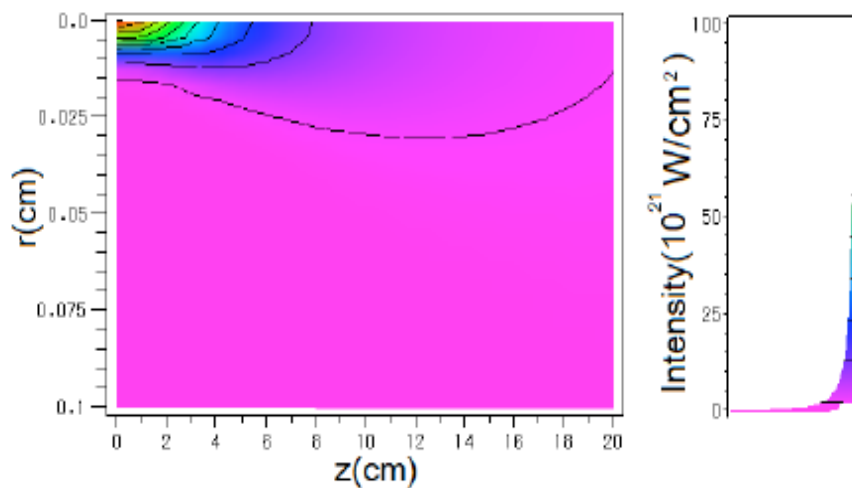


Figure 13. Contour of Gauss laser beam intensity in the reactor. (0,0) is a center position for focusing.



5. Energy Gain by the Reactions

This model is applied for D-D plasma. The energy from this nuclear reaction is produced as E_f from this simple model and can be written as

$$E_f = BQ Rr n_1 n_2 Vol t_L \tag{11}$$

Here, Q is energy from one event of nuclear reaction, n_1 and n_2 are number density as noted. Vol is a volume of region in length l with radius r_L of the laser focusing area, and t_L is the duration of laser pulse.

This is a kind of inertial confinement fusion. B is a burning rate of the fuel. During the active reaction time, the density of fuel is varied as

$$dn/dt = R n_0^2$$

and this can be written as

$$1/n - 1/n_0 = R t_0,$$

Here, t_0 is a characteristic time and is written as r_f/v_{pe} . v_{pe} is a perpendicular component of plasma particles velocity in a focused area. In this case, burning rate B is determined as

$$B = (n_0 - n)/n_0,$$

Then, B is rewritten as

$$B = R t_0 n_0 / (R t_0 n_0 + 1)$$

where t_0 is a confinement time of particles with cloud in plasma. This equation indicates the burning rate and comes to almost 1 by a simple estimation because the reaction rate is very large and thermal velocity is very small. Then, the gain of the energy G from the reactions is determined by

$$G = E_f/E_L \tag{12}$$

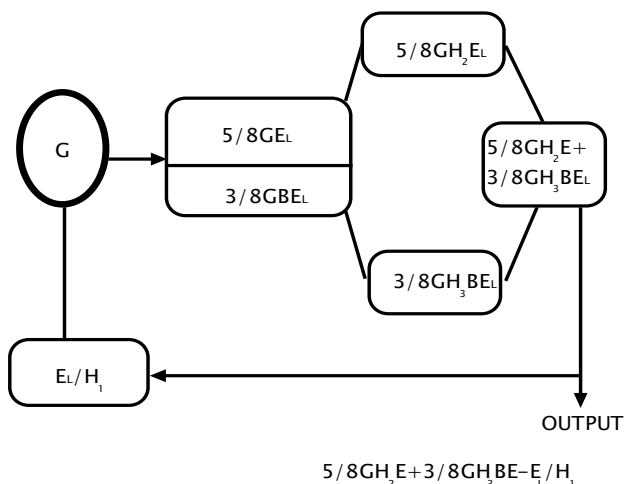
E_L is the laser energy in t_L of one pulse and can be written as $E_L = \pi r_L^2 I t_L$. When G is equal to 1.0, it is called break-even. Figure 9 shows gain obtained from Equation (12). In the case of Figure 13, the parameters that we used are summarized in Table 1. In an optimistic case, we can expect break-even around 100 kJ laser and can obtain gain 10 around several 100 kJ, although very high laser intensity with 10 ps pulse is required. When we use D-D reaction as a gain medium, hydrogen production by high temperature is possible in the reactor by this scheme [6].

6. Conceptual Reactor

6.1. Conceptual Reactor Configuration

The essential point of this article is to get efficient and economical energy with D-D reaction. For this purpose, we need an efficient reactor. Here we introduce a reactor to recover charged particles and neutrons produced by D-D reaction. Especially charged particle energy recovery is important for D-D reaction. Therefore, from this point of this view, the reactor for new laser fusion has a magnetic field to separate neutron and charged particles to have a high efficiency. In this reactor, we use a direct energy conversion of charged particles. High conversion efficiency with efficient laser makes an engineering break-even with low gain in the range of 10.

Figure 14. Schematic energy flow of the reactor with typical parameters.



Schematic energy flow of this reactor with typical parameters and the parameters are listed in Table 1. Blanket gain is an option in the actual case. The fuel in the case is deuterium, so charged particles play an important role when $B < 2$. When a larger blanket gain can be expected (more than 2), blanket material and gain is important. A depleted U or U_p burning to reduce the nuclear waist in the molten salt is conceivable and important issues for designing [8].

Table 1. Reactor parameters.

E_L	Laser energy of one shot	100–500 kJ
H_1	Efficiencies of Laser, conversion of	0.4
H_2	charged particles in reactor and	0.8
H_3	conversion of neutron in reactor	0.4
G	Gain by fusion reactions between deuterium	30
B	Blanket Gain of neutron Pu, Depleted U, Np, Long life chemical active FP	1–10

This reactor configuration has similarities to a mirror machine for magnetic confinement. Charged particles generated in the target as plasma are trapped in the magnetic field. They come out gradually through the end loss. A characteristic time is a few tens of a microsecond, although the burning time of high dense laser fusion target is much less than a nanosecond. A Larmor radius of energetic ions in the magnetic field is set to less than one-tenth of the radius of the mirror machine devices of this reactor, where the plasma is confined. Instabilities in this system should be considerable, but the efficiency for final conversion is not affected so strongly. Very low dense plasma is confined easily in the microsecond period because the density of the plasma is less than $10^{10}/\text{cm}^3$ when the target plasma is expanded and becomes uniform in this mirror magnetic field [4].

In this reactor, the charged particles are trapped by the magnetic field and are guided along the field. This causes the reduction of stress in the wall and blanket but the magnet coil obtains this. However, direct stress is reduced in strength and time significantly.

A ceramic laser has started to be developed. This shows a high laser gain, feasibility of large size scalability and high thermal conductivity. Even though the laser experiments have just started, this material shows several favorable features [6]. Figure 15 shows a schematic picture of this conceptual reactor. Energies from neutrons and charged particles are mainly produced at the center of this reactor by a D-D reaction and the following burning processes in the reactor. Most of the charged particle energy and little of the neutron energy is deposited in the plasma during inertial time. Neutrons and charged particles are separated by the magnetic field and deposit their energy in a blanket or direct converter, respectively. Several ways of direct conversion have been investigated [5]. The efficiency of direct conversion has been 70 to 90%.

Recent laser technology has allowed us to take the total efficiency of the laser system from 30 to 40% including electric power source. Such an efficient laser and direct conversion induce an engineering break-even with a low gain of target of 20 to 30 in this case.

A large part of the charged particles generated by the fusion reaction collide in the center plasma and

deposit their energy. This leads to the plasma expanding to fill the volume of the confinement region of 10 m^3 , although the target volume is 1 mm^3 . In this case, the expansion is occurred to be 10^{10} times, besides the time expansion of sub-ns burning time expands to microsecond confinement time with the end loss. Therefore, the particle in the end loss can be separated as a charged particle easily and converted into electric power directly.

Neutrons are scattered in the blanket as friction but this amount is three-eighths of the total energy. Most of the energy is deposited in the blanket of coolant and graphite or carbon compound. The combination of mirror machine and graphite blanket are expected to withstand a temperature of more than 800 K.

Neutron to thermal energy conversion is the most important issue in this design. The details of the simulation by neutron scattering are on the way. The rough estimation for a temperature of 800 K is assumed to get an efficient production. The temperature of blanket sets production efficiency about 50% by a simple model of Carnot's cycle.

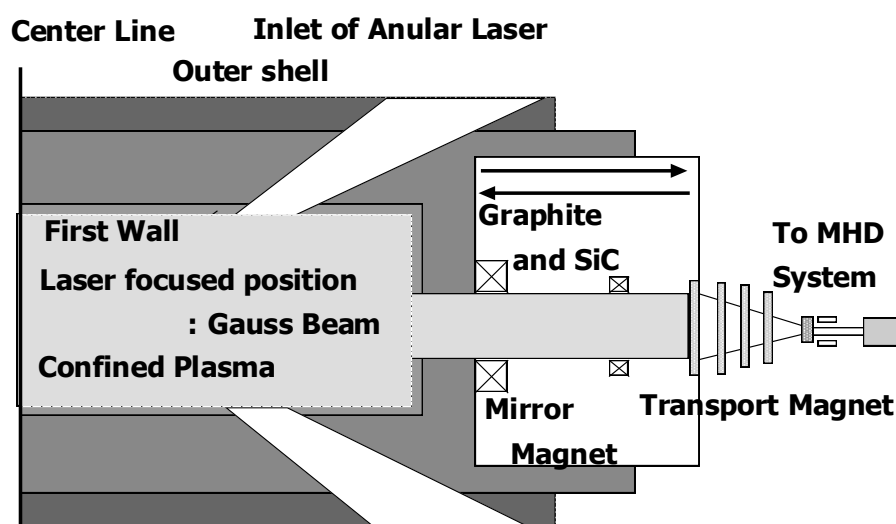
Blanket gain is optional with a hybrid fission blanket. Here we consider this reactor with a solid-state blanket of graphite for neutron energy capture. We can sustain the temperature high with enough safety.

For a graphite blanket, the temperature can reach 1000 K or more.

The first wall may be stainless steel. It is easy to replace economically after several years. After the replacement, it is stored for a long time to repose geologically. The structure material is SiC and graphite. The low Z with a simple structure makes low activation and can be replaced at appropriate time under regular investigation as fission reactor [6]. We can use it for the lifespan of the reactor. The advantage of graphite blanket is it exhibits low activation and, in the case of an accident, the released radioactivity is greatly reduced. The graphite may moderate the neutrons below activation energy levels.

The outer shell is concrete to withstand the high temperature and stress. This is covered and is supported by the reinforced concrete vessel. This also plays a role for neutron shielding.

Figure 15. Illustration of the reactor with mirror magnetic field and graphite solid blanket with molten salt coolant.



6.2. Reactor Parameters

The reactor parameters are listed in Table 2. The inner radius, which is as the first wall radius, the neutron density on the first wall should be chosen with 10 to 30 MW/m² for usual cases. However, in our case, the neutron density exceeded at the center part. We can replace the wall frequently here. The length is determined from the mirror magnet field. The mirror ratio of 10 is taken for a confinement of plasma and to obtain a conversion to electricity for a break-even. From conservative parameters, the length of 8 m is given. The blanket thickness for neutron energy deposition is calculated using Monte Carlo code of MCNP5, which is given.

Direct plasma energy converter is set on both sides of the reactor as a MHD energy converter. There are several methods for this. Here, we use a very simple and primitive one. The escaped plasma from the mirror end goes into the transport section of the length of several meters, in which plasma is transported and is focused to the end. Their motion is guided along the magnetic field. Finally, the charged particles convert most of their kinetic energy into an electric energy in this way.

A coolant candidate that we expect to use is molten salt. It is injected at 500 K from the outer layer and is heated gradually during the passage of each layer. Finally, the temperature is 1000 K at the first layer just before the first wall [7-10].

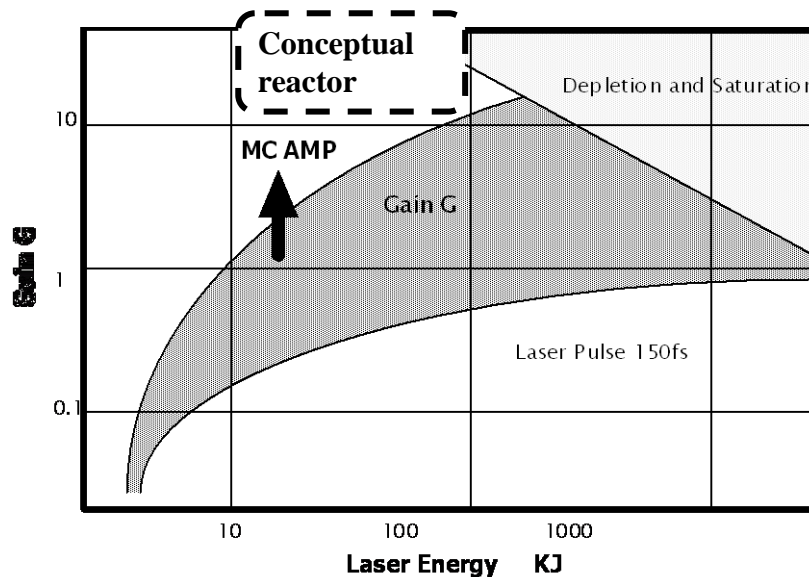
We add a simple mirror magnetic field to this reactor. This avoids a direct bombardment of charged particles on the first wall. As is well known, a mirror machine is a kind of amplifier that the possibility of amplification scheme in plasma is investigated. Here, we point out a possibility of amplification for denser plasma with smaller mirror field.

Table 2. Reaction parameters for gain in Deuteron reactor.

		Issues
Fuel for reaction	D-D, $[n + {}^3\text{He}]/[P + T] = 1/1$	Two plasma groups with Laser accelerated or plasma jet, <i>etc.</i>
Relative velocity of plasma particles	10^4 to 10^8 m/s	Slightly lower than the cut-off density of the laser
Density	$10^{21}/\text{cm}^3$	de Broglie wave group velocity
V_g	10^5 to 10^6 cm/s	$F = 0.3$
Laser intensity	$10^{24.5}$ W/cm ²	1 cycle 3 fs
$\langle t \rangle =$ laser pulse length or averaging duration of cloud	0.1 ps to 100 ps	Fermi-Dirac model
Nucleon Energy level around barrier foot	+1 keV to -5 keV	Diffraction Limit

A Gain curve including much uncertainty in the scheme is shown in Figure 16.

Figure 16. Gain of the reactor.



7. Conclusions

In this article, the feasibility of a new approach of laser fusion for break-even or above by Deuterium plasma is discussed. We found that the nuclear potential including mesons at the nuclear center plays an important role for tunneling of Coulomb potential of outer foot of Coulomb barrier, which had not been expected. The penetrability is significantly enhanced. We obtained a significant gain on this scheme and based on this, we designed a primitive reactor.

This is a new concept and consequently, there are many issues to be solved such as an optimal wave length, relation of Coulomb barrier and energy level of three dimensions, nucleon kinetic energy and so on. Adding these items, these are issues for

1. Saturation region on formation factor F .
2. Cloud behavior and lifespan.
3. Group velocity of nucleon and relative velocity of nucleon after tunneling.
4. Self-consistent field of Coulomb barrier region during the tunneling.
5. First wall structure to replace each several months.

Comments and your suggestion are very welcome.

Acknowledgements

We sincerely thank C. Yamanaka for his helpful suggestion and comments on this model and reactor.

References

1. Imasaki, K.; Li, D. An approach to laser induce nuclear fusion. *Laser Part. Beams* **2008**, *26*, 3–7.
2. Balantekin, A.; Takigawa, N. Quantum tunneling in Nuclear fusion. *Rev. Mod. Phys.* **1998**, *70*, 77–100.

3. Nuckolls, J.; Wood, L.; Thiessen, A.; Zimmerman, G. Laser compression of matter to super-high density. *Nature* **1972**, *239*, 139–143.
4. Lilley, J. *Nuclear Physics*; John Wiley & Sons: New York, NY, USA, 2001.
5. Li, D.; Imasaki, K.; Vacuum laser-driven accelerator by a slit-truncated Bessel beams. *Appl. Phys. Lett.* **2005**, *86*, 031110.
6. Borghesi, M.; Kar, S.; Romagnani, L.; Toncian, T.; Antici, P.; Audebert, P. Brambrink, E.; Ceccherini, F.; Cecchetti, C.A.; Fuchs, J.; Galimberti, M.; Gizzi, L.A.; Grismayer, T.; Lyseikina, T.; Jung, R.; Macchi, A.; Mora, P.; Osterholtz, J.; Schiavi, A.; Willi, O. Impulsive electric fields driven by high-intensity laser matter interactions. *Laser Part. Beams* **2007**, *25*, 161–167.
7. Shimada, Y.; Nisimura, H.; Nakai, M.; Yamanaka, C. Characterization of extreme ultraviolet emission from laser produced spherical tin plasma generated with multiple laser beams. *Appl. Phys. Lett.* **2005**, *86*, 051501.
8. Katoh, Y.; Kishimoto, H.; Kohyama, A. Fusion reactor structural materials. *J. Nucl. Mater.* **2002**, *307*, 1221.
9. Storm, E.; Latkowski, J.; Farmer, J.; Abbott, R.; Amendt, P.; Ankiam, T.; Caird, J.; Deri, R.; Erandson, A.; Kramer, K.; Loosmore, G.; Miles, R.; Fatel, P.; Serrano de Carro, M.; Shaw, F.; Tabak, M. Livermore group life. In Proceedings of the 6th IFSA, San Francisco, CA, USA, September 2009.
10. Imasaki, K.; Li, D. An approach to hydrogen production by inertial fusion energy *Laser Part. Beams* **2007**, *25*, 99–105.

© 2010 by the authors; licensee MDPI, Basel, Switzerland. This article is an Open Access article distributed under the terms and conditions of the Creative Commons Attribution license (<http://creativecommons.org/licenses/by/3.0/>).